New Physical Mechanisms in Laser Cooling

Y. Castin, K. Mølmer(*), J. Dalibard and C. Cohen-Tannoudji
College de France et Laboratoire de Spectroscopie Hertzienne de l'Ecole Normale Supérieure, 24 rue Lhomond, F-75231 Paris Cedex 05, France(**)

1. Introduction

Since the last Laser Spectroscopy Conference, there have been major advances in laser cooling. Two important limits have been overcome. First, precise measurements have shown that the temperatures in optical molasses were about one order of magnitude lower than the expected Doppler limit T_D given by $k_B T_D = \hbar\Gamma/2$, where Γ is the natural width of the excited state e (1-3). Simultaneously, it was shown that it is even possible to go below the recoil limit T_R given by $k_B T_R = \hbar^2k^2/2M$, where $\hbar^2k^2/2M$ is the recoil energy associated with the absorption or the emission of a single photon (4).

In this paper, we will focus on the new physical mechanisms allowing one to beat the Doppler limit. A first qualitative explanation of these mechanisms in terms of non-adiabatic effects for a multilevel atom moving in a gradient of laser polarization has been given independently by the Paris and Stanford groups at the last International Conference on Atomic Physics (2,3). We present here a few new theoretical results concerning polarization gradient cooling. After some general considerations on the connection between friction and non-adiabaticity (§2), we show in §3 that, in the simple case of 1-d molasses, there are two different cooling mechanisms which occur respectively when the two counterpropagating waves have orthogonal linear polarizations (lin $\perp$ lin case) or orthogonal circular polarizations (σ^+-σ^- case). A more detailed study of these two cases can be found in (5). We present here new velocity distribution profiles deduced from a full quantum treatment of atomic motion in the σ^+-σ^- configuration and we interpret the structures appearing in these profiles in terms of a large step momentum diffusion (§4).

2. General Considerations

An atom at rest in $\vec{r}$ has in general an internal steady state $\sigma_{st}(\vec{r})$ which depends on the characteristics of the laser electric field in $\vec{r}$ (amplitude, phase, polarization). Suppose now that the atom is moving with a velocity $\vec{v}$. Because of the finite internal response time τ_{int}, the internal state $\sigma(\vec{r}, \vec{v})$ for an atom passing in $\vec{r}$ with a velocity $\vec{v}$ lags behind $\sigma_{st}(\vec{r})$. These non-adiabatic effects are characterized by a dimensionless parameter $\epsilon = v\tau_{int}/\lambda = kv\tau_{int}$, which is the ratio between the distance travelled by the atom during τ_{int} and the laser wavelength $\lambda = 1/k$ which is the typical length scale for the laser field. The term linear in ϵ, in the perturbative expansion of $\sigma(\vec{r},v)$ in powers of ϵ, gives rise to a mean radiative force linear in v, $-\alpha v$, which can be interpreted as a friction force, α being the friction coefficient (6). On the other hand, general arguments using the connection between fluctuations and dissipation (7), allow one to relate the momentum diffusion coefficient D to α, and to show that the equilibrium temperature T of the atoms is given by

---

(*) Institute of Physics, University of Aarhus
DK-8000 Aarhus C. Denmark
(**) Laboratoire associé au C.N.R.S. et à l'Université Pierre et Marie Curie

$k_B T \sim D/M\alpha \geq \hbar/\tau_{int}$. When applied to a 2-level atom e-g, having a single internal time $\tau_{int} = \tau_R = 1/\Gamma$, which is the radiative lifetime of the excited state e, these general considerations lead to an equilibrium temperature $k_B T \sim \hbar/\tau_R = \hbar\Gamma$ which is nothing but the Doppler limit T_D.

Consider now an atom, such as an alkali atom, having several Zeeman sublevels in the ground state g. There is, in this case, new internal times τ_p, which are the mean optical pumping times between the Zeeman sublevels of g. We can write $\tau_p = 1/\Gamma'$, where Γ' is the mean scattering rate of the incident photons and can be considered as the radiative width of g due to the optical excitation. Note that such an optical excitation introduces also a light-shift $\hbar\Delta'$ of the Zeeman sublevels of g. At low laser intensity I_L, Γ' and Δ' are both proportional to I_L and can be much smaller than the natural width Γ of e. It follows that the new non-adiabaticity parameter $\epsilon' = kv\tau_p = kv/\Gamma'$ associated with τ_p can be much larger than the previous one $\epsilon = kv/\Gamma$. Non-adiabatic effects can thus appear at much lower velocities, giving rise to higher friction coefficients. The same general considerations predict also an equilibrium temperature $k_B T \gtrsim \hbar/\tau_p = \hbar\Gamma'$, much smaller than T_D, since $\Gamma' \ll \Gamma$ at low I_L.

Finally, let us discuss the importance of gradients of laser polarization. Since we want $\Gamma' \ll \Gamma$, the laser intensity must be small, so that the atom is mainly in g. On the other hand, non-adiabatic effects are important only if $\sigma_{st}(\vec{r})$ varies rapidly with $\vec{r}$. Since the total population in g is nearly equal to 1, and therefore independent of $\vec{r}$, the only possibility leading to large spatial gradients of $\sigma_{st}(\vec{r})$ is to have an anisotropy in g, usually described in terms of orientation or alignment, which depends strongly on $\vec{r}$. This can be achieved simply if the laser polarization varies rapidly in space.

3. The Two Types of Polarization Gradient Cooling at 1-Dimension

We summarize here the results derived in (5) in the simple case of 1-d molasses.

A first type of polarization gradient corresponds to a gradient of ellipticity with fixed polarization axis. It occurs for example when the two waves have equal amplitudes and orthogonal linear polarizations (lin $\perp$ lin configuration). In such a case, the polarization of the total field changes every $\lambda/8$ from σ^+, to linear, to σ^-, to linear, to σ^+... One can then show that the light-shifts and populations of the Zeeman sublevels of g are spatially modulated. For a moving atom, optical pumping between these sublevels gives rise to a "Sisyphus effect" analogous to the one occuring in stimulated molasses (8,9) : because of the finite optical pumping time, the atom can climb a potential hill and reach the top of this hill before being optically pumped to a potential valley. During the climbing, part of the kinetic energy is transformed into potential energy, the decrease of atomic momentum being due to the dipole forces, or, equivalently, to a redistribution of photons between the two counterpropagating waves. On the other hand, the energy dissipation, which is essential for the cooling process, is achieved by spontaneous anti-Stokes Raman processes, which carry away the potential energy gained during the climbing.

The second type of polarization gradient corresponds to a pure rotation of the polarization axis, with a fixed ellipticity. It occurs for example when the two counterpropagating waves have equal amplitudes and orthogonal circular polarizations (σ^+-σ^- configuration). In such a case, the resulting polarization is always linear and rotates around the propagation axis Oz of the two waves, forming an helix with a pitch λ. Since the laser intensity is independent of z, the light-shifts of the Zeeman sublevels in g remain constant in space, so that no dipole forces can exist in this case. A new

cooling mechanism occurs if there are more than two Zeeman sublevels in g ($J_g \geq 1$) and is due to the fact that the wave functions of the light-shifted sublevels in g vary in space. More precisely, one can show that, even at very low velocity, atomic motion in a rotating linear polarization produces a population difference between the Zeeman sublevels in g defined along Oz, giving rise to a large imbalance between the radiation pressures exerted by the two counterpropagating waves. This imbalance varies as kv/Δ', where $\hbar\Delta'$ is the light-shift splitting in g, and is due to a contamination of the wave functions in g induced by atomic motion. It is much larger than the corresponding imbalance occuring for Doppler cooling and which varies as kv/Γ. Let us mention finally that, in the $\sigma^+-\sigma^-$ configuration, the energy dissipation is not due to anti-Stokes Raman processes. In steady state, there are as many Stokes as anti-Stokes processes. As in Doppler cooling, the energy dissipation is due to the fact that, on the average, the fluorescence photons have a blue Doppler shift.

All the previous results are derived from a semi-classical theory, where the position $\vec{r}$ of the atom is treated as a classical variable, and are summarized (for $|\delta| \geq \Gamma$) in the table 1. The temperature achievable by polarization gradient cooling is predicted to be proportional to the laser power (5). This could suggest that one can reach arbitrarily low temperature by using sufficiently low laser power. Actually, this is not true : the previous semi-classical approach is valid only if the atomic de Broglie wavelength remains small compared to the laser wavelength λ, or, in other words, if the atomic kinetic energy remains large compared to the recoil energy. This imposes a lower limit on the laser power range that can be studied semi-classically. Below this limit, a full quantum approach has to be developped. The outline of such an approach is presented in the next section.

	2-level	Lin ⊥ Lin	$\sigma_+-\sigma_-$
Capture range	$kv \simeq -\delta$	$kv \simeq \Gamma'$	$kv \simeq -\Delta'$
Friction α	$-\hbar k^2 \frac{\Gamma'}{\delta}$	$-\hbar k^2 \frac{\Delta'}{\Gamma'}$	$-\hbar k^2 \frac{\Gamma'}{\Delta'}$
Diffusion D	$\hbar^2 k^2 \Gamma'$	$\hbar^2 k^2 \Gamma' \frac{\Delta'^2}{\Gamma'^2}$	$\hbar^2 k^2 \Gamma'$
Temperature $k_B T = \frac{D}{\alpha}$	$-\hbar\delta$	$-\hbar\Delta'$	$-\hbar\Delta'$

Table 1. Predictions of the semi-classical theory for the Doppler cooling of a 2-level atom, and for the two polarization gradient coolings discussed here. The detuning $\delta = \omega_L - \omega_0$ is negative and large compared to Γ, so that the light shift Δ' is also negative and large compared to Γ'. For simplicity, numerical factors have been omitted.

4. Quantum treatment of atomic motion in the σ_+-σ_- case

Such a treatment uses a quantum description of both internal and external degrees of freedom. This amounts to consider the following density matrix elements

$$< e \text{ or } g,\ m,\ p_x,\ p_y,\ p_z \ |\rho|\ e \text{ or } g,\ m',\ p'_x,\ p'_y,\ p'_z > \qquad (1)$$

where m and m' stand for the Zeeman sublevels indices and p_x, p'_x, ... for the cartesian components of the atomic momentum.

The evolution of ρ is given by the generalized optical Bloch equations including recoil (10,11). Consequently, once the laser field configuration is known, the problem is in principle solvable at least numerically. However, it requires a very large size of computer memory ($(8 \times 10^6) \times (8 \times 10^6)$ array for a $J_g = 1 \leftrightarrow J_e = 2$ transition with 100 steps in p along each direction) and we have not performed such a 3-dimensional quantum analysis. On the other hand, the 1-dimensional case is much less memory consuming especially for the σ_+-σ_- case as we show now.

In this latter case indeed, conservation of angular momentum implies that many non-diagonal matrix elements of the type of (1) are zero in the stationary state. Consider for example the following family of states :

$$\mathcal{F}(p) = \left\{ |g,\ m,\ p + m\hbar k>;\ |e,\ m',\ p + m'\hbar k > \right\}$$

$$\text{with } |m| \leqslant J_g \qquad |m'| \leqslant J_e = J_g + 1$$

The laser atom interaction only couples the states of this family to states belonging to the same family. For instance, the atom in the state $|g,\ m = -1,\ p - \hbar k >$ can absorb a σ_+ photon (momentum $\hbar k$) and go to the state $|e,\ m = 0,\ p >$. There, it can emit a σ_+ stimulated photon and jumps into the state $|g,\ m = 1,\ p + \hbar k >$ and so on... On the other hand, since there is a perfect correlation between the direction $\pm\hbar k$ of the photons and their angular momentum, two states belonging to two different families cannot be connected by absorption-stimulated emission processes. Only spontaneous emission can cause population transfers between families, but it cannot build any off-diagonal density matrix element between two states belonging to two different families.

This important remark considerably reduces the number of non-zero density matrix elements to be considered. For example, for a $1 \leftrightarrow 2$ transition with 100 steps in p, this number is only $800 \times 8 = 6400$ which is easy to deal with on a reasonable size computer.

Two ways can be used to find the stationary state of the atomic density operator. The first one is to calculate the time evolution of the density matrix elements and to wait for a long enough time. The second way is to solve directly the equation $\dot{\rho} = 0$ by a matrix inversion. We have checked that the two methods lead to similar results, the latter being the fastest one.

Examples of results are given in fig. 1, representing four stationary momentum distributions. These curves have been calculated for a Cesium type atom (atomic mass 133, resonant wavelength 852 nm, resonant transition linewidth $\Gamma/2\pi = 5$ MHz). The parameters of the atom laser interaction are the same for the four curves (Rabi frequency $0.5\ \Gamma$, detuning $\delta = -3\Gamma$). The only change between the four calculations concerns the angular momenta of the atomic levels involved in the cooling process, from $J_g = 1 \rightarrow J_e = 2$ (curve a) to $J_g = 4 \rightarrow J_e = 5$ (curve d, corresponding to the real situation for Cesium).

These four curves exhibit qualitatively the same types of features : narrow peak around p = 0 with a width of a few recoil, superimposed on a

much broader pedestal. The relative size of the narrow peak with respect to the pedestal depends strongly of the angular momenta of the transition, the pedestal being more important when J_g and J_e increase.

Let us now discuss briefly the origin of these two features. First, the narrow peak appears to have characteristics very close to the Gaussian predicted by the semi-classical model, at least if the power is not too low so that the width of the semi-classical Gaussian remains much larger than the recoil momentum.

We think that the large pedestal originates from an anomalous momentum diffusion appearing at high velocities and due to correlations between the directions of two successively absorbed photons. Indeed, because of optical pumping, after the absorption of a σ_+ photon, the atom has a high probability to be in a state $|g, m\rangle$ with a high value m of J_z. Because of the Clebsch-Gordan coefficients, it has then a higher probability to absorb another σ_+ photon than a σ_- one, the difference between these probabilities increasing with J_g. It follows that the atom absorbs in sequence several σ_+ photons, then several σ_- ones, and so on..., thus performing a large step random walk in p-space, the size of the steps increasing with J_g (5, 12, 13).

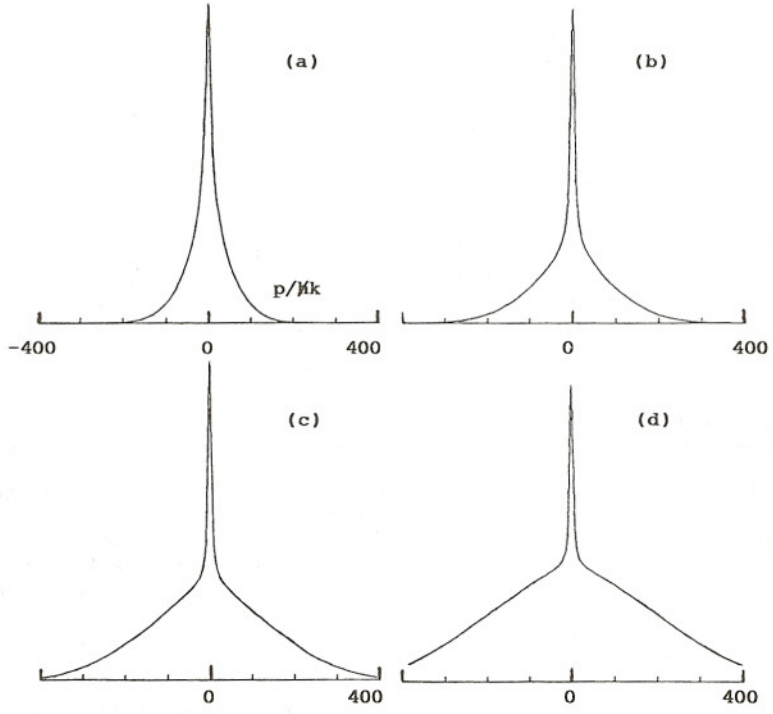

Fig. 1. Stationary momentum distributions in the σ_+-σ_- configuration, calculated from a full quantum theory of atomic motion. The parameters are the same for the 4 curves (see text) except for the angular momenta J_g and $J_e = J_g+1$: (a) : $J_g = 1$, (b) : $J_g = 2$, (c) : $J_g = 3$, (d) : $J_g = 4$.

Such an enhancement of the momentum diffusion coefficient D occurs only if the eigenstates of J_z can be considered as stationary between two fluorescence cycles, i.e. on a time scale $\tau_p = 1/\Gamma'$. This is achieved either for a moving atom with $kv \gg |\Delta'|$ or for a slow atom if the detuning is small ($kv \leqslant |\Delta'|$, $|\delta| \leqslant \Gamma$). Otherwise, for example if $kv \simeq 0$ and $|\delta| \gg \Gamma$, the correlations between successive absorptions is destroyed by a complete redistribution of populations among the various Zeeman sublevels. Such a redistribution is due to absorption-stimulated emission processes which, for an atom at rest, have a rate $|\delta|/\Gamma$ larger than spontaneous processes.

Using these results, it is then possible to understand, at least qualitatively, the momentum profiles of fig. 1. Around $v = 0$, the anomalous diffusion is small and the friction force is important, giving rise to a narrow structure. For larger velocities, the diffusion coefficient D increases (this increase being more important for large J_g and J_e). This gives rise to the large pedestals of fig. 1.

We are now working on the extension of this quantum calculation to more general laser configurations.

References

(1) P. Lett, R. Watts, C. Westbrook, W.D. Phillips, P. Gould and H. Metcalf, Phys. Rev. Lett. 61, 169 (1988)

(2) J. Dalibard, C. Salomon, A. Aspect, E. Arimondo, R. Kaiser, N. Vansteenkiste and C. Cohen-Tannoudji, in *Atomic Physics 11*, S. Haroche, J.C. Gay and G. Grynberg eds, World Scientific 1989, p. 199

(3) a. S. Chu, D.S. Weiss, Y. Shevy and P.J. Ungar, in *Atomic Physics 11*, same reference as in (2), p. 636

b. Y. Shevy, D.S. Weiss, P.J. Ungar and S. Chu, Phys. Rev. Lett. 62, 1118 (1989)

(4) a. A. Aspect, E. Arimondo, R. Kaiser, N. Vansteenkiste and C. Cohen-Tannoudji, Phys. Rev. Lett. 61, 826 (1988)

b. Same authors, to appear in J.O.S.A. B, 1989, Special Issue on Laser Cooling and Trapping

(5) J. Dalibard and C. Cohen-Tannoudji, to appear in J.O.S.A. B, 1989, Special Issue on Laser Cooling and Trapping

(6) J.P. Gordon and A. Ashkin, Phys. Rev. A21, 1606 (1980)

(7) J. Dalibard and C. Cohen-Tannoudji, J. Phys. B18, 1661 (1985)

(8) J. Dalibard and C. Cohen-Tannoudji, J.O.S.A. B2, 1707 (1985)

(9) A. Aspect, J. Dalibard, A. Heidmann, C. Salomon and C. Cohen-Tannoudji, Phys. Rev. Lett. 57, 1688 (1986)

(10) S. Stenholm, Appl. Phys. 16, 159 (1978)

(11) C. Bordé in *Advances in Laser Spectroscopy*, F.T. Arecchi, F. Strumia and H. Walther eds, Plenum, 1983

(12) Y. Castin and K. Mølmer, to be published

(13) P.J. Ungar, D.S. Weiss, E. Riis and S. Chu, to appear in J.O.S.A. B, 1989, Special Issue on Laser Cooling and Trapping.